

Heterogeneous Fenton process optimization with $\text{Ni}_{0.5}\text{Zn}_{0.5}\text{Fe}_2\text{O}_4$ nanocatalyst in stabilized landfill leachate treatment

Otimização do processo Fenton heterogêneo com nanocatalisador $\text{Ni}_{0.5}\text{Zn}_{0.5}\text{Fe}_2\text{O}_4$ no tratamento de lixiviado estabilizado de aterro sanitário

Amanda Gondim Cabral Quirino¹ , Joelda Dantas¹ , Arthur Marinho Cahino¹ , Iana Chaiene de Araujo Vidal¹ ,
Fabiana Costa Bezerra¹ , Elisângela Maria Rodrigues Rocha¹ 

ABSTRACT

Landfill leachates are highly complex and recalcitrant effluents, exhibiting high pollution potential when not subjected to proper treatment. The heterogeneous Fenton process with $\text{Ni}_{0.5}\text{Zn}_{0.5}\text{Fe}_2\text{O}_4$ nanocatalyst was applied to optimize the decolorization of stabilized raw landfill leachate, considering the color number in terms of the spectral absorption coefficient. For this, the central composite design (CCD) and the response surface methodology (RSM) were used to optimize the operating parameters: pH, catalyst concentration, and H_2O_2 factor. $\text{Ni}_{0.5}\text{Zn}_{0.5}\text{Fe}_2\text{O}_4$ catalyst was characterized by X-ray diffraction (XRD), Fourier transform infrared spectroscopy (FTIR), textural analysis using the Brunauer–Emmett–Teller and the Barrett–Joyner–Halenda (BET–BJH) method, scanning electron microscopy (SEM), and dynamic light scattering (DLS). According to the analysis of variance (ANOVA), the model generated by experimental data regression was statistically significant, with a coefficient of determination (R^2) of 0.96. The optimal point defined by the response surfaces corresponded to the values of H_2O_2 factor 1.14, pH 8.02, and catalyst concentration 0.66 g L^{-1} , whose combination of values resulted in a theoretical response of 89.70% decolorization of the leachate. The validation tests revealed an excellent fit between the value predicted by the model and the values obtained experimentally. The reproducibility of the optimized condition is limited to stabilized leachates. Under the optimized condition, the heterogeneous Fenton process, when compared to the isolated H_2O_2 and $\text{Ni}_{0.5}\text{Zn}_{0.5}\text{Fe}_2\text{O}_4$ processes, provided higher absorbance removals of simple and conjugated aromatic compounds, as well

RESUMO

Lixiviados de aterros sanitários são efluentes de elevada complexidade e recalcitrância, apresentando alto potencial poluidor quando não submetidos a tratamentos adequados. O processo Fenton heterogêneo com nanocatalisador $\text{Ni}_{0.5}\text{Zn}_{0.5}\text{Fe}_2\text{O}_4$ foi aplicado para otimizar a descoloração de lixiviado estabilizado *in natura* de aterro sanitário, considerando-se o número de cor em termos do coeficiente de absorção espectral. Para isso, foram utilizados o delineamento composto central rotacional (DCCR) e a metodologia de superfície de resposta (MSR) para a otimização dos parâmetros operacionais: pH, concentração de catalisador e fator de H_2O_2 . O catalisador $\text{Ni}_{0.5}\text{Zn}_{0.5}\text{Fe}_2\text{O}_4$ foi caracterizado por difração de raios X (DRX), espectroscopia no infravermelho por transformada de Fourier (FTIR), análise textural pelo método BET–BJH, microscopia eletrônica de varredura (MEV) e espalhamento dinâmico de luz (DLS). De acordo com a análise de variância (ANOVA), o modelo gerado pela regressão dos dados experimentais foi estatisticamente significativo, com coeficiente de determinação (R^2) de 0,96. O ponto ótimo definido pelas superfícies de resposta correspondeu aos valores de 1,14 de fator de H_2O_2 , 8,02 de pH e $0,66 \text{ g L}^{-1}$ de concentração de catalisador, cuja combinação de valores resultou na resposta teórica de 89,70% de descoloração do lixiviado. Os testes de validação revelaram excelente ajuste entre o valor predito pelo modelo e os valores obtidos experimentalmente. A reprodutibilidade da condição otimizada limita-se aos lixiviados estabilizados. Na condição otimizada, o processo Fenton heterogêneo, quando comparado aos processos isolados H_2O_2 e $\text{Ni}_{0.5}\text{Zn}_{0.5}\text{Fe}_2\text{O}_4$, proporcionou maiores remoções de absorbância de compostos aromáticos simples e conjugados, como

¹Federal University of Paraíba – João Pessoa (PB), Brazil.

Corresponding author: Amanda Gondim Cabral Quirino – Federal University of Paraíba – Postgraduate Program in Civil and Environmental Engineering – Campus I – CEP: 58051-900 – João Pessoa (PB), Brazil. E-mail: amandagcq@hotmail.com

Conflicts of interest: the authors declare no conflicts of interest.

Funding: Coordination for the Improvement of Higher Education Personnel – Brazil (CAPES) – Finance Code 001, Paraíba State Research Foundation (FAPESQ), grant number 3147/2021, and National Postdoctoral Program (PNPD/CAPES) – 24001015072P9 – Renewable Energies, Call No. 03/2018.

Received on: 10/16/2024. Accepted on: 07/07/2025.

<https://doi.org/10.5327/Z2176-94782311>



This is an open access article distributed under the terms of the Creative Commons license.

as the integrated spectral area from 200 to 800 nm, thus revealing its effectiveness in the treatment of landfill leachate, considering the parameters analyzed, and its contribution to achieving the Sustainable Development Goals (SDGs).

Keywords: Ni-Zn ferrite; decolorization; analysis of variance; response surface methodology; advanced oxidation process.

Introduction

Population growth and the expansion of cities lead to an increase in the amount of solid waste generated, leading to the expansion of landfills, which are one of the main methods of final waste disposal in many parts of the world (Sossou et al., 2024).

The disposal of solid waste in landfills has environmental, social, and economic implications. The adverse environmental effects of this practice involve the production of methane, a potent greenhouse gas, and the generation of leachate, an effluent with a high potential for contaminating water bodies. Additionally, landfills present the risk of surface fires or subterranean combustion, which can lead to atmospheric pollution (Gutberlet and Bramryd, 2025). Due to their economic viability, landfills are often chosen in the context of solid waste management (Nguyen et al., 2025). Especially in developing countries, a part of this management is carried out by waste pickers, who collect and divert materials that would otherwise be sent to landfills, but this service is not well remunerated (Gutberlet and Bramryd, 2025). It should be noted, however, that well-managed landfills bring environmental, social, and economic gains through the proper treatment of leachate, energy recovery, and job creation (Gutberlet and Bramryd, 2025; Nguyen et al., 2025; Nouri; Al-Khatib, 2025).

In landfills, there is a combination of physical (precipitation, percolation, runoff, infiltration, and evaporation), chemical (oxidation, complexation, and dissolution), and biological (acetogenesis, methanogenesis, and nitrification) processes that transform solid waste into a wide variety of compounds, and generate landfill leachate, which is composed of dissolved organic matter, inorganic components, heavy metals, and xenobiotic organic compounds (Wijekoon et al., 2022).

The discharge of landfill leachate without appropriate treatment can cause soil, surface, and groundwater pollution, directly or indirectly affecting human health, ecosystems, food chains, and environmental safety (Ma et al., 2018; Guo et al., 2021). Most of the refractory organic matter present in landfill leachate has high aromaticity and is in the form of dissolved organic matter with a high molecular weight, consisting mainly of humic and fulvic acids. The high complexity and low biodegradability of leachate make it difficult to treat using conventional biological processes (Guo et al., 2021; Taşci et al., 2021).

também de área espectral integrada de 200 a 800 nm, revelando, portanto, sua efetividade no tratamento de lixiviado de aterro sanitário, considerando-se os parâmetros analisados e sua contribuição para o alcance dos Objetivos de Desenvolvimento Sustentável (ODS).

Palavras-chave: ferrita Ni-Zn; descoloração; análise de variância; metodologia de superfície de resposta; processo oxidativo avançado.

Advanced oxidation processes (AOPs) are particularly suitable for treating refractory wastewater with a high concentration of pollutants and low biodegradability ratios, such as landfill leachate (Ma et al., 2018; Guo et al., 2024). AOPs generate high concentrations of free radicals, including the hydroxyl radical ($\bullet\text{OH}$), which is a strong oxidant capable of decomposing most complex organic molecules into simpler substances (Metcalf and Eddy, 2016).

The Fenton process is a classical AOP, whose reaction mechanism was initially proposed in its homogeneous form, in which H_2O_2 undergoes a series of chain reactions with Fe^{2+} in solution, producing $\bullet\text{OH}$ radicals to degrade organic pollutants. The Fenton method is non-selective, simple, low in toxicity, and can be applied under ambient temperature and pressure conditions (Guo et al., 2024). However, homogeneous Fenton requires an acidic initial pH, and the added Fe^{2+} generates iron-rich sludge, causing secondary pollution. To overcome the limitations of the classic homogeneous Fenton process, solid iron-based catalysts have been used alternatively, thus consisting of heterogeneous Fenton systems (Li et al., 2024). In heterogeneous Fenton processes, the pH working range is wider, and the reaction to produce $\bullet\text{OH}$ from H_2O_2 takes place on the surface of the catalysts, which can be easily recovered after the reactions, avoiding the formation of iron-rich sludge (Pham et al., 2018; Sruthi et al., 2018; Turk and Asci, 2023).

The heterogeneous Fenton process applied to the treatment of landfill leachate has been investigated using various catalysts, including studies employing pure iron (Ertugay et al., 2017; Chen et al., 2018; Bogacki et al., 2019; Tejera et al., 2019), as well as those using multimetallic catalysts containing iron (Ma et al., 2018; Pham et al., 2018; Sruthi et al., 2018; Niveditha and Gandhimathi, 2020b; Guo et al., 2021). The heterogeneous Fenton technology has proven to be promising and effective in the treatment of landfill leachate through research carried out in different countries. However, there is a need for investigations into its reproducibility at a pilot scale, further analysis of the composition of the organic matter in the leachate after the processes, and the use of low-cost heterogeneous catalysts (Quirino et al., 2022).

In conducting a bibliometric and systematic review, Quirino et al. (2022) found that most of the optimized conditions for heterogeneous Fenton processes applied to landfill leachate treatment have been determined using the one-factor-at-a-time method, meaning that interac-

tions among the variables influencing the process were not considered. Furthermore, the authors observed a predominance of contributions from Indian and Chinese researchers, with a noticeable lack of applications of the heterogeneous Fenton process to landfill leachate treatment in the Brazilian context.

In the national context, the study conducted by Moretti et al. (2023) addressed the application of the heterogeneous solar photo-Fenton process using Zn-Mn ferrite for the treatment of landfill leachate with an initial chemical oxygen demand (COD) of $1,600 \text{ mg L}^{-1}$. The authors found that the heterogeneous solar photo-Fenton process was effective in treating the leachate only when combined with physicochemical coagulation as a pre-treatment. This indicates the incipience of research focused on leachates from Brazilian landfills, highlighting the urgent need for investigations into the heterogeneous Fenton technology using different solid catalysts and their application to leachates with varying levels of recalcitrance. Therefore, to contribute to the advancement of knowledge, the present study investigated the heterogeneous Fenton process using $\text{Ni}_{0.5}\text{Zn}_{0.5}\text{Fe}_2\text{O}_4$ for the treatment of a more recalcitrant Brazilian landfill leachate, with an initial COD of $9,000 \text{ mg L}^{-1}$.

The ferrite $\text{Ni}_{0.5}\text{Zn}_{0.5}\text{Fe}_2\text{O}_4$ presents several advantages for environmental applications, such as effective pilot-scale production, cost-effective synthesis, high specific surface area, which enhances the availability of active sites, strong affinity for various pollutants, and high thermal and chemical stability (Dantas et al., 2021b; Tahar et al., 2024).

Thus, the objective of the present study was to optimize the heterogeneous Fenton process using the $\text{Ni}_{0.5}\text{Zn}_{0.5}\text{Fe}_2\text{O}_4$ nanocatalyst for the decolorization of stabilized raw landfill leachate, considering the color number (CN) in terms of the spectral absorption coefficient (SAC). Optimization was performed using a central composite design (CCD) combined with response surface methodology (RSM), considering the synergistic effects of the input variables (pH, catalyst concentration, and H_2O_2 factor) to determine the optimal point.

Therefore, the scope of this work is directly aligned with the Sustainable Development Goals (SDGs), significantly contributing to SDG 6 (Clean Water and Sanitation) by promoting the treatment of a complex effluent. Additionally, the use of advanced technology with a nanocatalyst reinforces SDG 9 (Industry, Innovation, and Infrastructure) by driving innovation in the environmental sanitation sector.

Materials and methods

Collection and characterization of landfill leachate

Leachate was collected from the decantation pond of the Metropolitan Sanitary Landfill of João Pessoa ($7^\circ 13' 5.33''\text{S}$ and $34^\circ 57' 22.86''\text{W}$), located in the State of Paraíba, Northeast Region of Brazil. This landfill has been in operation since 2003. The samples collected from the decantation pond corresponded to raw effluent and were characterized according to American Public Health Association (APHA) (APHA et al., 2012) methods.

Catalyst preparation and characterization

$\text{Ni}_{0.5}\text{Zn}_{0.5}\text{Fe}_2\text{O}_4$ ferrite nanoparticles were synthesized using a combustion reaction according to Dantas et al. (2021a) and characterized by X-ray diffraction (XRD), Fourier-transform infrared spectroscopy (FTIR), textural analysis by nitrogen adsorption using the Brunauer–Emmett–Teller (BET) method, scanning electron microscopy (SEM), and dynamic light scattering (DLS).

For the synthesis of $\text{Ni}_{0.5}\text{Zn}_{0.5}\text{Fe}_2\text{O}_4$, the oxidizing reagents used were nickel nitrate hexahydrate ($\text{Ni}(\text{NO}_3)_2 \cdot 6\text{H}_2\text{O}$), zinc nitrate hexahydrate ($\text{Zn}(\text{NO}_3)_2 \cdot 6\text{H}_2\text{O}$), and iron(III) nitrate nonahydrate ($\text{Fe}(\text{NO}_3)_3 \cdot 9\text{H}_2\text{O}$), while urea ($\text{CO}(\text{NH}_2)_2$) was employed as the fuel and reducing agent. The initial composition of the solution was based on the total valence of the oxidizing and reducing agents, according to the principles of propellant and explosive chemistry. The redox mixture of metal nitrates and fuel was subjected to direct heating in a conical reactor designed for pilot-scale combustion synthesis, with a production capacity of 200 g per batch. The nanocatalyst was obtained as porous flakes, which were deagglomerated using a porcelain mortar and pestle, and sieved through a 325 mesh ($45 \mu\text{m}$). To ensure reproducibility of the synthesis, seven batches were prepared, yielding 1 kg of $\text{Ni}_{0.5}\text{Zn}_{0.5}\text{Fe}_2\text{O}_4$ nanocatalyst. The formation of the major crystalline phase was confirmed in all syntheses through structural analysis.

XRD analysis was performed using a Bruker D2 Phaser diffractometer ($\text{Cu-K}\alpha$ radiation), operated at 40 kV and 30 mA . The crystallite size was calculated using the Diffrac.Eva software, based on the broadening of the XRD line (d_{311}), by deconvolution of the secondary diffraction line of polycrystalline cerium (used as a standard), using the Scherrer equation (Klung and Alexander, 1962). Crystallinity was determined from the ratio between the integrated area of the peak corresponding to the crystalline phase and the area for the amorphous phase.

The FTIR spectrum was recorded in the range of $4,000\text{--}650 \text{ cm}^{-1}$, with a resolution of 4 cm^{-1} and 20 scans, using a Bruker Vertex 70 spectrometer. To observe the characteristic bands of the analyzed material, the FTIR spectrum was plotted in the expanded region from 900 to 200 cm^{-1} .

The specific surface area of the catalyst was determined by nitrogen adsorption using the BET method. Analyses were performed in triplicate using a Micromeritics NOVA 3200 instrument. The average equivalent diameter was calculated using Equation 1 (Reed, 1996):

$$D_{\text{BET}} = \frac{6}{S_{\text{BET}} \rho} \quad (1)$$

Where:

D_{BET} : the average equivalent diameter (nm);

S_{BET} : the specific surface area determined by the BET method ($\text{m}^2 \text{ g}^{-1}$);

ρ : the theoretical density (g cm^{-3});

6: a theoretical factor adopted for spherical particles.

Pore volume and pore diameter were determined according to the method developed by Brunauer, Joyner, and Halenda (BJH).

SEM was used to investigate the morphological properties of the $\text{Ni}_{0.5}\text{Zn}_{0.5}\text{Fe}_2\text{O}_4$ catalyst. The sample was analyzed using a Tescan Vega3 scanning electron microscope.

Particle size was determined by DLS using a HORIBA Scientific nanoparticle analyzer, SZ-100 series, operating in the range of 10–10,000 nm. DLS measures fluctuations in the intensity of scattered light over time. For the analysis, 0.10 g of the sample was dispersed using a 50% silica solution as a deflocculant.

Heterogeneous Fenton treatment

Heterogeneous Fenton ($\text{Ni}_{0.5}\text{Zn}_{0.5}\text{Fe}_2\text{O}_4/\text{H}_2\text{O}_2$) process experiments were conducted at the bench scale using 100 mL of stabilized raw landfill leachate. All assays were performed in the dark in 250 mL beakers placed on a SOLAB SL 180/D orbital shaker table to ensure rapid mixing at 100 rpm. The process time was 150 min, and the experiments were carried out at ambient temperature and pressure. The $\text{Ni}_{0.5}\text{Zn}_{0.5}\text{Fe}_2\text{O}_4$ catalyst and H_2O_2 were added according to the conditions of each experiment. The pH of the leachate samples was adjusted using 6 N H_2SO_4 . The assays aimed to determine the optimal conditions for leachate decolorization, considering the operational variables pH, $\text{Ni}_{0.5}\text{Zn}_{0.5}\text{Fe}_2\text{O}_4$ concentration, and H_2O_2 concentration.

Leachate decolorization was evaluated based on the CN, as defined by Equation 2. The CN is based on the SAC (in cm^{-1}) in the visible range, measured at wavelengths of 436, 525, and 620 nm. The SAC (Equation 3) was determined from the absorbance (Abs) of the sample using a 1 cm path length cuvette (Tizaoui et al., 2007; Primo et al., 2008), through spectral scanning performed with a Hach DR 6000 UV-Visible spectrophotometer. The experimental efficiencies were calculated according to Equation 4, where CN_i and CN_f correspond to the CN values before and after the heterogeneous Fenton treatment, respectively.

$$\text{CN} = \frac{\text{SAC}_{436}^2 + \text{SAC}_{525}^2 + \text{SAC}_{620}^2}{\text{SAC}_{436} + \text{SAC}_{525} + \text{SAC}_{620}} \quad (2)$$

$$\text{SAC}_i = \frac{\text{Abs}_i}{l} \quad (3)$$

$$\text{Ef. (\%)} = \left(\frac{\text{CN}_i - \text{CN}_f}{\text{CN}_i} \right) \times 100 \quad (4)$$

Process optimization

The CCD and RSM were employed as optimization techniques for the heterogeneous Fenton process. The concentration of the $\text{Ni}_{0.5}\text{Zn}_{0.5}\text{Fe}_2\text{O}_4$ catalyst, the H_2O_2 factor, and pH were defined as independent variables, while the leachate decolorization efficiency was adopted as the response variable. All independent variables were coded at five levels: -1.68, -1, 0, +1, and +1.68 (Table 1), and a total of 17 experiments were conducted, including eight factorial points, six axial points, and three replicates at the central point.

Table 1 – Independent variables and coded levels of the 2³ CCD.

Independent variables	Symbols	Coded levels				
		-1.68	-1	0	+1	+1.68
pH	X_1	2.98	4.00	5.50	7.00	8.02
Catalyst concentration (g L^{-1})	X_2	0.66	1.00	1.50	2.00	2.34
H_2O_2 factor	X_3	0.33	0.50	0.75	1.00	1.17

Each experiment had its H_2O_2 concentration determined based on the COD of the stabilized raw landfill leachate ($9,000 \text{ mg O}_2 \text{ L}^{-1}$) and the H_2O_2 factor associated with the experiment, according to Equation 5 (Moravia, 2010). The investigated range comprised from 33 to 117% of the H_2O_2 amount relative to the stoichiometric quantity of O_2 required for complete COD stabilization. Therefore, the H_2O_2 concentration tested varied from $6,311.25 \text{ mg L}^{-1}$ (0.19 mol L^{-1}) to $22,376.25 \text{ mg L}^{-1}$ (0.66 mol L^{-1}).

$$[\text{H}_2\text{O}_2] = \text{H}_2\text{O}_2 \text{ factor} \times 2.125 \times \text{COD}_{\text{raw landfill leachate}} \quad (5)$$

The statistical analysis of the results involved developing a mathematical model where the response variable, decolorization, was expressed as a function of the input variables and their interactions, considering only those statistically significant at a 5% significance level and following the hierarchy principle. The second-order polynomial equation was generated based on Equation 6, where Y is the response, a_0 is the average of the responses, and a_i , a_{ij} , and a_{ijk} are the response coefficients. The second term in the equation represents the linear effects, the third term represents the second-order effects, and the fourth term accounts for the interactions (Chelladurai et al., 2021).

$$Y = a_0 + \sum_{i=1}^k a_i x_i + \sum_{i=1}^k a_{ii} x_i^2 + \sum_{i,j=1, j \neq i}^k a_{ij} x_i x_j \quad (6)$$

To evaluate the quality of fit of the generated model, the coefficient of determination (R^2) and analysis of variance (ANOVA) were employed, where the F-value was determined. The optimized condition was identified using the desirability method. Finally, the proposed model was experimentally validated in triplicate under the optimized condition.

Under the optimized condition, the spectral response of the leachate to the heterogeneous Fenton process and the individual processes (H_2O_2 alone and $\text{Ni}_{0.5}\text{Zn}_{0.5}\text{Fe}_2\text{O}_4$ alone) was investigated. For this purpose, the absorbances of simple aromatic compounds (at wavelengths of 228, 254, and 284 nm) and conjugated aromatic compounds (at 310 nm) were considered, according to Colombo et al. (2018). Additionally, the integrated spectral area from 200 to 800 nm was determined based on Equation 7 (Correa et al., 2020; Neves et al., 2020).

$$A_{200-800} = \int_{200}^{800} f(x) dx \quad (7)$$

Where:

$A_{200-800}$: Integrated spectral area from 200 to 800 nm;

$f(x)$: Absorbance curve function from 200 to 800 nm.

Results and Discussion

Characterization of the leachate

The physicochemical characterization of the leachate is summarized in Table 2. According to the classification proposed by Wijekoon et al. (2022), the leachate can be classified as mature, stabilized, or methanogenic, due to its age >10 years, its $\text{pH} > 7.50$, and its biodegradability ratio, as indicated by biochemical oxygen demand ($\text{BOD}_{5,20}/\text{COD} < 0.10$), which suggests the presence of humic and fulvic substances in the effluent. The low $\text{BOD}_{5,20}/\text{COD}$ ratio (0.05) indicates that the leachate cannot be effectively treated using biological processes, making AOPs more suitable (Sruthi et al., 2018).

Catalyst characterization

In the XRD pattern of the $\text{Ni}_{0.5}\text{Zn}_{0.5}\text{Fe}_2\text{O}_4$ ferrite (Figure 1), the predominant presence of Ni-Zn nanoferrite was observed, following the standard JCPDS card no. 52-0278. Additionally, characteristic peaks corresponding to segregated phases of hematite (Fe_2O_3) and zinc oxide (ZnO) were identified, which may potentially contribute beneficially to the reactions by acting as active metals and promoters. The structural data indicated a crystallinity of $56.80 \pm 1.6643\%$ and a crystallite size of 36.93 ± 1.3576 nm, respectively. The diffraction profile confirmed the successful synthesis of $\text{Ni}_{0.5}\text{Zn}_{0.5}\text{Fe}_2\text{O}_4$ by the combustion method, as evidenced by the predominant formation of the expected main phase and its nanoscale dimension, a feature favorable for catalytic applications. Harzali and Azizi (2024) also synthesized $\text{Ni}_{0.5}\text{Zn}_{0.5}\text{Fe}_2\text{O}_4$ and reported the presence of the characteristic peaks of this type of ferrite, with the main peak at $2\theta = 35.5^\circ$, in agreement with Wang et al. (2024).

Table 2 – Physicochemical characterization of stabilized raw landfill leachate.

Parameters (units)	Values
Total alkalinity ($\text{mg CaCO}_3 \text{L}^{-1}$)	10,914.00
Ammonia ($\text{mg N-NH}_3 \text{L}^{-1}$)	2,260.55
Chlorides (mg Cl L^{-1})	3,998.76
Color (mg Pt-Co L^{-1})	8,912.90
$\text{BOD}_{5,20}$ ($\text{mg O}_2 \text{L}^{-1}$)	456.75
COD ($\text{mg O}_2 \text{L}^{-1}$)	9,000.00
$\text{BOD}_{5,20}/\text{COD}$	0.05
Nitrate ($\text{mg N-NO}_3 \text{L}^{-1}$)	0.11
pH	8.02
Total solids (mg L^{-1})	37,782.00
Total fixed solids (mg L^{-1})	32,305.00
Total volatile solids (mg L^{-1})	5,477.00
Sulfate ($\text{mg SO}_4 \text{L}^{-1}$)	113.60
Turbidity (NTU)	277.00

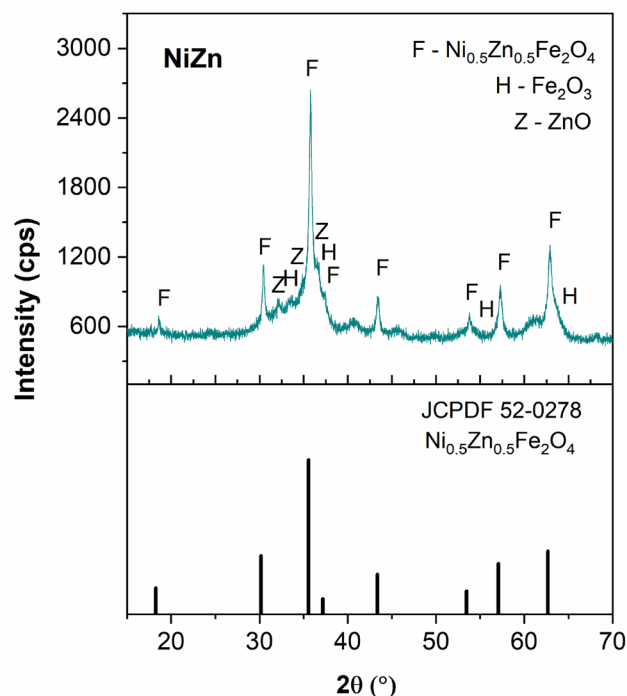


Figure 1 – X-ray diffraction pattern of $\text{Ni}_{0.5}\text{Zn}_{0.5}\text{Fe}_2\text{O}_4$ ferrite.

Figure 2a shows the infrared vibrational spectrum in the range of $900\text{--}200 \text{ cm}^{-1}$ for the $\text{Ni}_{0.5}\text{Zn}_{0.5}\text{Fe}_2\text{O}_4$ ferrite. The presence of absorption bands below $1,000 \text{ cm}^{-1}$ is verified, which are characteristic of ferrites with a spinel-type crystalline structure. Additionally, two absorption bands are observed in the frequency range of $200\text{--}750 \text{ cm}^{-1}$, which are typical of AB_2O_4 spinel structures. These bands are associated with the vibrations of divalent and trivalent ions within the crystal lattice. The absorption band ν_2 , located around 550 cm^{-1} , is attributed to the vibrations of tetrahedral sites, while the ν_1 band, located around 300 cm^{-1} , corresponds to the vibrations of octahedral sites (Tahar et al., 2024).

The N_2 adsorption/desorption isotherms of the $\text{Ni}_{0.5}\text{Zn}_{0.5}\text{Fe}_2\text{O}_4$ ferrite are shown in Figure 2b. The catalyst exhibited a type IV isotherm, suggesting mesoporous characteristics of the material, along with a type H3 hysteresis loop (Oliveira and Andrada, 2019). Table 3 compiles the BET and BJH parameters for the $\text{Ni}_{0.5}\text{Zn}_{0.5}\text{Fe}_2\text{O}_4$ catalyst, obtained from triplicate analyses. The results revealed an average equivalent diameter of 17.44 ± 0.29 nm, with a ratio between the equivalent diameter and the crystallite size of less than 1, indicating the nanoscale dimension of the synthesized ferrite. The mesoporous characteristic of the $\text{Ni}_{0.5}\text{Zn}_{0.5}\text{Fe}_2\text{O}_4$ catalyst was confirmed by SEM (Figure 3). The SEM micrographs reveal the heterogeneous morphology of the material, composed of irregular particle agglomerates. The presence of these agglomerates supports the previously discussed results since a smaller average equivalent diameter corresponds to a larger surface area and a higher degree of particle aggregation. Mapossa et al. (2020) synthesized $\text{Ni}_{0.5}\text{Zn}_{0.5}\text{Fe}_2\text{O}_4$ by com-

bustion reaction and also obtained the catalyst at the nanoscale, with an average equivalent diameter of 15 ± 0.41 nm. These authors likewise identified agglomerates with various shapes and sizes, consistent with the $\text{Ni}_{0.5}\text{Zn}_{0.5}\text{Fe}_2\text{O}_4$ micrographs shown in Figure 3.

Table 4 presents the particle diameter sizes of $\text{Ni}_{0.5}\text{Zn}_{0.5}\text{Fe}_2\text{O}_4$ ferrite obtained by DLS, according to the particle size distribution indexes D (10%), D (50%), and D (90%), respectively. The D (10%) and D (90%) parameters refer to the cutoff diameters of the cumulative distribution curve at 10 and 90%, respectively, while the D (50%) parameter corresponds to the median of the distribution and represents the mean particle diameter (D_m). Thus, the particle size determined by DLS confirmed that the catalyst was obtained at the nanoscale, with an average diameter of 40.55 ± 0.22 nm. The particle size values obtained are in agreement with Dantas et al. (2021b), who reported a D (10%) of 26 nm, a D (50%) of 39.6 ± 1.8 nm, and a D (90%) of 63.2 nm for $\text{Ni}_{0.5}\text{Zn}_{0.5}\text{Fe}_2\text{O}_4$ ferrite synthesized by combustion reaction.

Heterogeneous Fenton process optimization

The analytical results of leachate decolorization (Y) using the heterogeneous Fenton process are presented in Table 5, along with the coded and real values of the input variables associated with each experiment.

The highest decolorization efficiency of stabilized raw landfill leachate achieved was 69.48%, obtained through the combination of pH 7, a catalyst concentration of 2 g/L, and an H_2O_2 factor equal to 1. Tejera et al. (2019) also investigated the treatment of landfill leachate by the heterogeneous Fenton process with different $[\text{H}_2\text{O}_2]/[\text{COD}]$ ratios: 2.125 (factor 1), 1.063 (factor 0.5), and 0.531 (factor 0.25), and similarly found that the highest decolorization efficiency was obtained with an H_2O_2 factor equal to 1 and pH equal to 7.

To optimize the process and achieve maximum leachate decolorization efficiency, statistical data analysis was conducted. The use of the 2^3 CCD in the investigation of the heterogeneous Fenton process enabled the development of a mathematical model; that is, it became possible to express the response variable, decolorization, as a function of the interfering variables in the process. The second-order polynomial mathematical model of the response variable decolorization as a function of the interfering variables is presented in Equation 8, where Y(X) is the decolorization efficiency (%), X_1 is the pH, X_2 is the $\text{Ni}_{0.5}\text{Zn}_{0.5}\text{Fe}_2\text{O}_4$ catalyst concentration (g L^{-1}), and X_3 is the H_2O_2 factor.

$$Y(X) = -64.9 + 9.1 X_1 - 5.2 X_2 + 96.7 X_3 - 0.36 X_1^2 + 3.45 X_2^2 - 84.4 X_3^2 - 0.93 X_1 X_2 + 12.11 X_1 X_3 \quad (8)$$

The coefficients of the linear terms in Equation 8 revealed that X_1 and X_3 had a positive effect on leachate decolorization; that is, increases in variables X_1 and X_3 caused an increase in response Y. However, the negative coefficient of X_2 indicated that increasing variations in this variable tended to reduce Y. The negative coefficients of the quadratic terms X_1^2 and X_3^2 indicated the existence of maximum points; in other words, beyond certain values, further increases in X_1^2 and X_3^2 resulted in a decrease in response Y. The opposite effect was observed for X_2^2 since this term presented a positive coefficient and, therefore, a minimum point. The negative coefficient of the interaction between X_1 and X_2 revealed that the combined effect of pH and catalyst concentration is antagonistic. Conversely, the positive coefficient of the interaction between X_1 and X_3 indicated a synergy between the variables pH and H_2O_2 factor. These results revealed the complexity of the studied system and the importance of using a coded equation to analyze the effects of variables and their interactions, as highlighted by Niveditha and Gandhimathi (2020b).

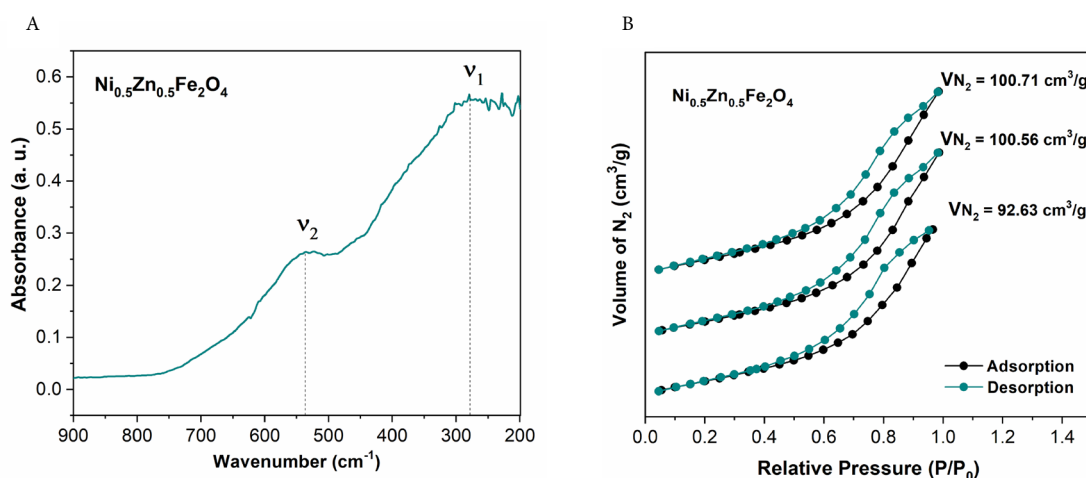


Figure 2 – (a) FTIR spectrum of $\text{Ni}_{0.5}\text{Zn}_{0.5}\text{Fe}_2\text{O}_4$ ferrite, and (b) N_2 adsorption/desorption isotherms of $\text{Ni}_{0.5}\text{Zn}_{0.5}\text{Fe}_2\text{O}_4$ ferrite, in triplicate.

Table 3 – BET and BJH parameter values for $\text{Ni}_{0.5}\text{Zn}_{0.5}\text{Fe}_2\text{O}_4$ ferrite.

Sample	S_{BET} ($\text{m}^2 \text{g}^{-1}$)	D_{BET} (nm)	V_p ($\text{cm}^3 \text{g}^{-1}$)	R_p (Å)	D_{BET}/T_c
$\text{Ni}_{0.5}\text{Zn}_{0.5}\text{Fe}_2\text{O}_4$	64.17 ± 1.07	17.44 ± 0.29	0.152 ± 0.01	32.63 ± 5.12	0.47

S_{BET} : specific surface area; D_{BET} : average equivalent diameter; V_p : pore volume; R_p : pore radius; T_c : crystallite size.

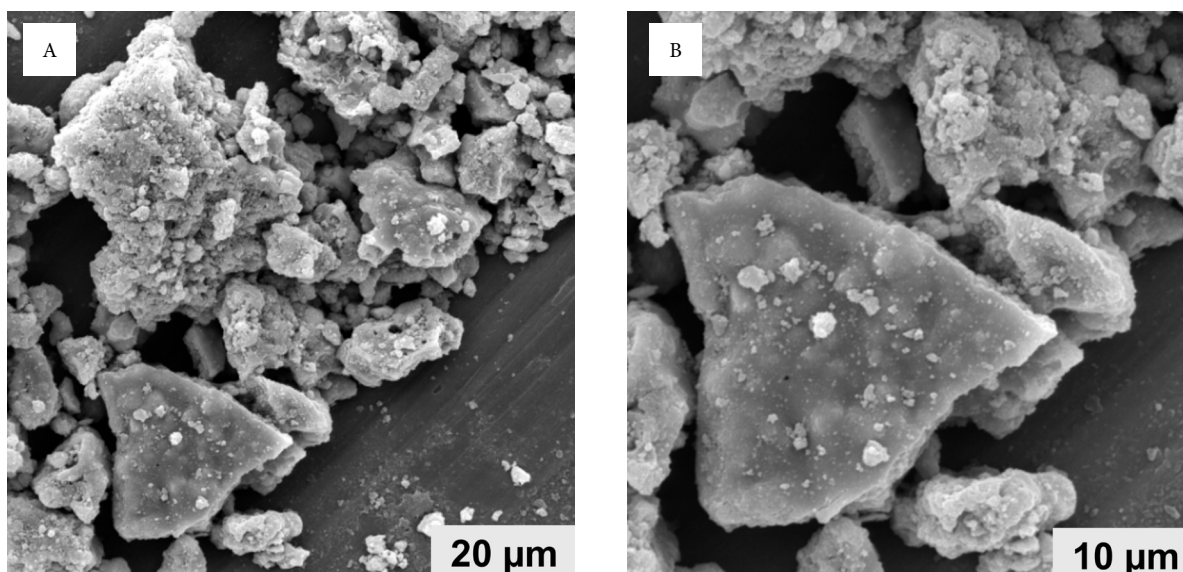


Figure 3 - Morphologies observed by SEM for $\text{Ni}_{0.5}\text{Zn}_{0.5}\text{Fe}_2\text{O}_4$ ferrite: (a) 20 μm and (b) 10 μm .

Table 4 – Particle diameters of $\text{Ni}_{0.5}\text{Zn}_{0.5}\text{Fe}_2\text{O}_4$ ferrite obtained by DLS, according to the distribution indexes.

Sample	D (10%) nm	D (50%) nm	D (90%) nm
$\text{Ni}_{0.5}\text{Zn}_{0.5}\text{Fe}_2\text{O}_4$	27.27	40.55±0.22	62.53

ANOVA (Table 6) was used to assess the statistical quality of the generated quadratic model. According to the model's coefficient of determination ($R^2=0.96$) and the ratio $F_{\text{cal}}/F_{\text{tab}}=6.92$, the proposed model showed a satisfactory fit to the experimental responses since $R^2>0.75$ and $F_{\text{cal}}/F_{\text{tab}}>4$ (Myers et al., 2016). For the terms of a model to be statistically significant, it must present a p-value less than 0.05 and a high F-value in the ANOVA (Guo et al., 2021; Taşci et al., 2021). Thus, according to the ANOVA (Table 6), all model terms were statistically significant, except for the linear component of the catalyst concentration variable. The linear component of the pH variable showed the most statistically significant effect on leachate decolorization, with the highest F-value and the lowest p-value. The linear and quadratic components of the H_2O_2 factor were the second and third most significant terms, respectively, followed by the interaction between pH and the H_2O_2 factor. The remaining model terms showed less influence on the decolorization response.

The response surfaces associated with the mathematical model generated by the regression of the experimental data from the 2^3 CCD are illustrated in Figure 4. According to Guo et al. (2021), response surfaces are useful for visualizing the ANOVA results. As observed in Figures 4a and 4b, the increase in pH led to a rapid increase in the decolorization of the landfill leachate, reinforcing the statistically significant and positive effect of pH on the response. Furthermore, Figure 4a highlights the statistically significant inter-

action between pH and the H_2O_2 factor, in which these variables were able to synergistically enhance the process efficiency. As reported in the ANOVA, the catalyst concentration showed a lower influence on the response, corroborating the behavior observed in Figures 4b and 4c.

Within the studied range, the optimal point defined by the response surfaces for the decolorization of the stabilized raw landfill leachate by the heterogeneous Fenton process corresponded to the following values: H_2O_2 factor=1.14, pH=8.02, and catalyst concentration=0.66 g L^{-1} , whose combination resulted in a theoretical decolorization efficiency of 89.70%.

Chen et al. (2018) applied the heterogeneous photo-Fenton process with Fe^0 catalyst for the treatment of landfill leachate pretreated by a combined anoxic/oxic-membrane bioreactor-reverse osmosis process, and determined the optimal condition of 0.5 g L^{-1} catalyst concentration, 20 mL L^{-1} H_2O_2 concentration, and pH 2, resulting in 88.30% decolorization and 85.69% UV_{254} removal from the leachate. Meanwhile, Niveditha and Gandhimathi (2020a) used flyash augmented Fe_3O_4 catalyst to treat stabilized raw landfill leachate by the heterogeneous Fenton process and obtained 68.7% UV_{254} removal under the optimized condition of 1 g L^{-1} catalyst concentration, 0.05 M H_2O_2 concentration, and pH 3.

In the present investigation, the finding that the best performance of the heterogeneous Fenton process using the $\text{Ni}_{0.5}\text{Zn}_{0.5}\text{Fe}_2\text{O}_4$ catalyst occurred at alkaline pH, corresponding to the natural pH value of the leachate (8.02), facilitates the feasibility of the treatment since it is not necessary to acidify the leachate before the application of the process. This characteristic was highlighted by Pham et al. (2018) as one of the advantages of the heterogeneous Fenton process.

Table 5 – Conditions of the independent variables and the experimental response of the 2^3 CCD used in the heterogeneous Fenton process ($\text{Ni}_{0.5}\text{Zn}_{0.5}\text{Fe}_2\text{O}_4/\text{H}_2\text{O}_2$) for the treatment of stabilized raw landfill leachate, with the reaction time set at 150 min.

Experiments	Independent variables						Response
	pH (X_1)		Catalyst concentration (X_2)		H_2O_2 factor (X_3)		Decolorization (Y)
	Coded	Real	Coded	Real (g L^{-1})	Coded	Real	%
1	-1	4.00	-1	1.00	-1	0.50	12.43
2	-1	4.00	-1	1.00	1	1.00	17.48
3	-1	4.00	1	2.00	-1	0.50	18.12
4	-1	4.00	1	2.00	1	1.00	19.02
5	1	7.00	-1	1.00	-1	0.50	47.52
6	1	7.00	-1	1.00	1	1.00	68.63
7	1	7.00	1	2.00	-1	0.50	48.31
8	1	7.00	1	2.00	1	1.00	69.48
9	-1.68	2.98	0	1.50	0	0.75	09.12
10	1.68	8.02	0	1.50	0	0.75	66.78
11	0	5.50	-1.68	0.66	0	0.75	45.22
12	0	5.50	1.68	2.34	0	0.75	40.12
13	0	5.50	0	1.50	-1.68	0.33	02.48
14	0	5.50	0	1.50	1.68	1.17	48.13
15 (C)	0	5.50	0	1.50	0	0.75	42.44
16 (C)	0	5.50	0	1.50	0	0.75	41.78
17 (C)	0	5.50	0	1.50	0	0.75	41.59

Table 6 – Analysis of variance (ANOVA) for the quadratic model generated for the response variable decolorization of stabilized raw landfill leachate by the heterogeneous Fenton process ($\text{Ni}_{0.5}\text{Zn}_{0.5}\text{Fe}_2\text{O}_4/\text{H}_2\text{O}_2$).

Source	SS	Df	MS	F_{cal}	p	F_{tab}	$F_{\text{cal}}/F_{\text{tab}}$	R^2
Model	6,797.36	8	849.67	23.81	0.000	3.44	6.92	0.96
X_1 – pH	5,097.22	1	5,097.22	25,616.77	0.000			
X_2 – $\text{Ni}_{0.5}\text{Zn}_{0.5}\text{Fe}_2\text{O}_4$	0.01	1	0.01	0.03	0.877			
X_3 – H_2O_2 factor	1,144.37	1	1,144.37	5,751.16	0.000			
X_1^2	7.36	1	7.36	36.98	0.026			
X_2^2	8.36	1	8.36	42.03	0.023			
X_3^2	313.96	1	313.96	1,577.86	0.001			
X_1X_2	3.89	1	3.89	19.54	0.048			
X_1X_3	165.05	1	165.05	829.49	0.001			
Residual	285.42	8	35.67					
Corrected total	7082.79	16						

SS: sum of squares; df: degrees of freedom; MS: mean squares; F_{cal} : $F_{\text{calculated}}$; F_{tab} : $F_{\text{tabulated}}$; R^2 : coefficient of determination.

The highest H_2O_2 concentration investigated in the experimental design was 0.66 mol L^{-1} (factor 1.17) and, according to the response surfaces, the optimal H_2O_2 factor value was 1.14, corresponding to $0.64 \text{ mol H}_2\text{O}_2 \text{ L}^{-1}$. This result is justified by the negative coefficient of the quadratic term of the H_2O_2 factor variable, which indicates the existence of a maximum point that, once exceeded, caused a decrease in the response. A similar trend was observed in other studies, such as those by Ma et al. (2018), Niveditha and Gandhimathi (2020a, 2020b), and Sruthi et al. (2018), where

the H_2O_2 variable showed a positive effect on the heterogeneous Fenton processes up to a certain limit value and, when surpassed, the effect became negative. These authors attributed this behavior to the scavenging of $\bullet\text{OH}$ radicals and, consequently, to the generation of hydroperoxyl radicals ($\text{HO}_2\bullet$), formed by the reaction between excess H_2O_2 and $\bullet\text{OH}$ radicals. The $\text{HO}_2\bullet$ radical has a lower oxidation potential than $\bullet\text{OH}$ and is oxidized to water and oxygen, with such effects being responsible for reducing the process efficiency at H_2O_2 concentrations above the optimal value.

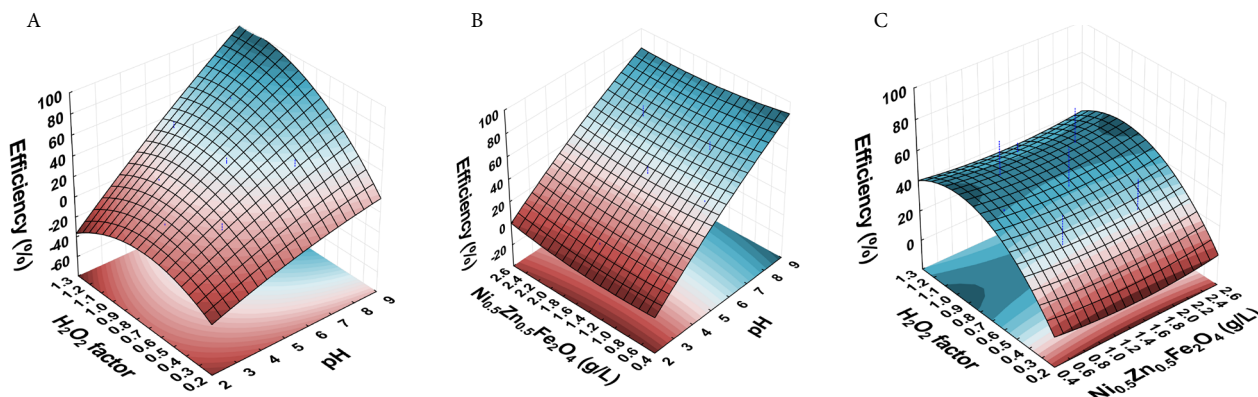


Figure 4 – Response surfaces for the leachate decolorization efficiency as a function of: (a) pH and H_2O_2 factor, (b) pH and catalyst concentration, and (c) catalyst concentration and H_2O_2 factor.

The investigated catalyst concentration range comprised values from 0.66 to 2.34 g L^{-1} . The optimization process results revealed that the analytical response for leachate decolorization is maximized at 0.66 g L^{-1} , the lowest value studied, which was probably caused by the anticatalytic effect that excess catalyst can cause in the system, as the iron present may act as a scavenger of $\bullet\text{OH}$ radicals, potentially limiting the reactions between $\bullet\text{OH}$ radical species and pollutants, resulting in decreased color removal from the leachates (Ma et al., 2018; Niveditha and Gandhimathi, 2020a, 2020b).

Among the advantages of the heterogeneous Fenton process, one of the most notable is its wide pH operating range, which allows the system to function under neutral and alkaline pH conditions (He et al., 2016). This was confirmed in the present investigation, with an optimal pH value of 8.02, corresponding to the natural pH of the leachate, as illustrated by the response surfaces (Figure 4). High efficiencies in the heterogeneous Fenton system were also obtained by Pham et al. (2018) under neutral and alkaline pH conditions when investigating the removal of oxytetracycline from landfill leachate using the $\text{H}_2\text{O}_2/\text{Cu}@ \text{Fe}_3\text{O}_4$ system, with removal efficiencies for the pharmaceutical in the leachate of 97.90 and 93.50% at pH values of 7.22 and 9.05, respectively.

The optimized condition (H_2O_2 factor=1.14, pH=8.02, and $\text{Ni}_{0.5}\text{Zn}_{0.5}\text{Fe}_2\text{O}_4$ catalyst concentration=0.66 g L^{-1}) was experimentally validated through triplicate assays, and the experimental responses obtained were compared with the response predicted by the model (89.70%). The results of the triplicate from the validation experiment are presented in Table 7.

Table 7 – Experimental responses from the validation assays and model-predicted response under the optimized condition (H_2O_2 factor=1.14, pH=8.02, and $\text{Ni}_{0.5}\text{Zn}_{0.5}\text{Fe}_2\text{O}_4$ catalyst concentration=0.66 g L^{-1}).

Assay	Experimental (%)	Predicted (%)	Error (±%)	SD (±%)	CV (%)
1	85.55	89.70	4.62	2.93	3.35
2	86.20		3.90	2.47	2.81
3	86.84		3.19	2.02	2.29

SD: standard deviation; CV: coefficient of variation.

The optimization process was validated due to the low values of errors (<4.62%), standard deviations (<2.93%), and coefficients of variation (<3.35%) between the model-predicted value and the experimental values (Lucena et al., 2019; Niveditha and Gandhimathi, 2020b). Figure 5 illustrates the visual aspect of the samples obtained in the experimental validation assays of the model.

Comparison with other processes under the optimized condition

At the optimal point for leachate decolorization by the heterogeneous Fenton process ($\text{Ni}_{0.5}\text{Zn}_{0.5}\text{Fe}_2\text{O}_4/\text{H}_2\text{O}_2$), two other processes were investigated: H_2O_2 alone and $\text{Ni}_{0.5}\text{Zn}_{0.5}\text{Fe}_2\text{O}_4$ ferrite alone. Colombo et al. (2018) used the absorbance of simple and conjugated aromatic compounds to assess the treatment efficiency of different processes applied to a raw landfill leachate with recalcitrant characteristics and a low biodegradability ratio ($\text{BOD}_5/\text{COD}=0.33$). The photo-Fenton process achieved absorbance removal rates of 58, 64, 62, and 66% at wavelengths of 228, 254, 284, and 310 nm, respectively. Higher absorbance removal rates were obtained in the present investigation using the heterogeneous Fenton process, considering the same wavelengths: 68.64, 69.06, 72.40, and 75.09%, respectively.

As shown in Figure 6, among the processes investigated, the heterogeneous Fenton process ($\text{Ni}_{0.5}\text{Zn}_{0.5}\text{Fe}_2\text{O}_4/\text{H}_2\text{O}_2$) provided the highest removal of absorbance related to simple and conjugated aromatic compounds, as well as the greatest reduction of the integrated spectral area from 200 to 800 nm. The removal efficiency for all analyzed parameters followed the order: $\text{Ni}_{0.5}\text{Zn}_{0.5}\text{Fe}_2\text{O}_4/\text{H}_2\text{O}_2 > \text{H}_2\text{O}_2 > \text{Ni}_{0.5}\text{Zn}_{0.5}\text{Fe}_2\text{O}_4$. A similar behavior was observed by Niveditha and Gandhimathi (2020b) when comparing the efficiency of the heterogeneous Fenton process ($\text{FeMoPO}/\text{H}_2\text{O}_2$) with the individual processes using only H_2O_2 and only FeMoPO for the treatment of landfill leachate, where the order was: $\text{FeMoPO}/\text{H}_2\text{O}_2 > \text{H}_2\text{O}_2 > \text{FeMoPO}$. The authors attributed the removal achieved using only the FeMoPO catalyst to the adsorption process, which likely also occurred in the present study with $\text{Ni}_{0.5}\text{Zn}_{0.5}\text{Fe}_2\text{O}_4$. The removals obtained in experiments using only H_2O_2 are due to the presence of iron in the leachates, which reacts with H_2O_2 to generate hydroxyl radicals (Niveditha and Gandhimathi, 2020b).

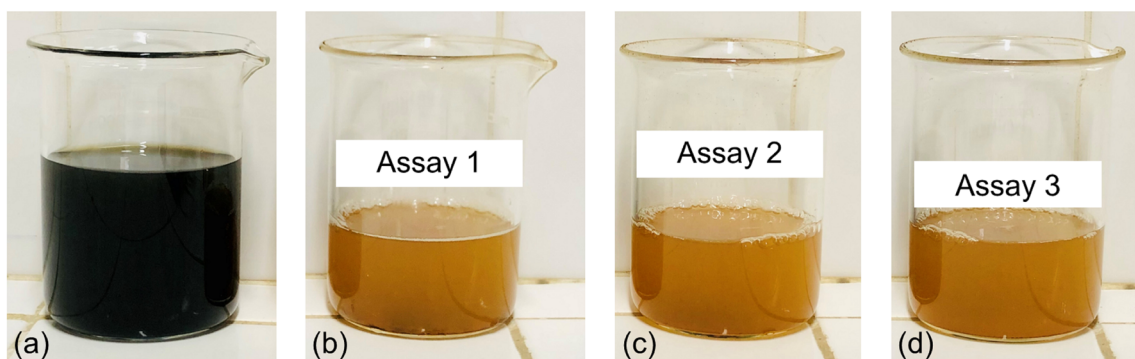


Figure 5 – (a) Stabilized raw landfill leachate, and (b, c, d) leachate treated by the heterogeneous Fenton process under the optimized condition (H_2O_2 factor=1.14, $\text{pH}=8.02$, and $\text{Ni}_{0.5}\text{Zn}_{0.5}\text{Fe}_2\text{O}_4$ catalyst concentration= 0.66 g L^{-1}) for 150 min, in triplicate.

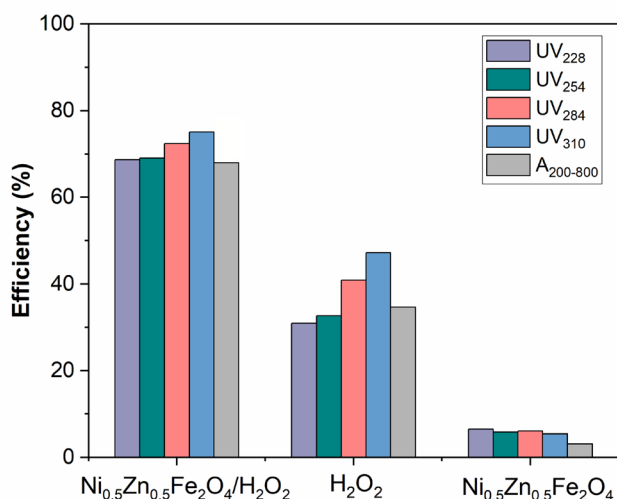


Figure 6 – Comparison of processes for the removal of simple aromatic compounds (absorbances at 228, 254, and 284 nm), conjugated aromatic compounds (310 nm), and integrated spectral area from 200 to 800 nm in stabilized raw landfill leachate.

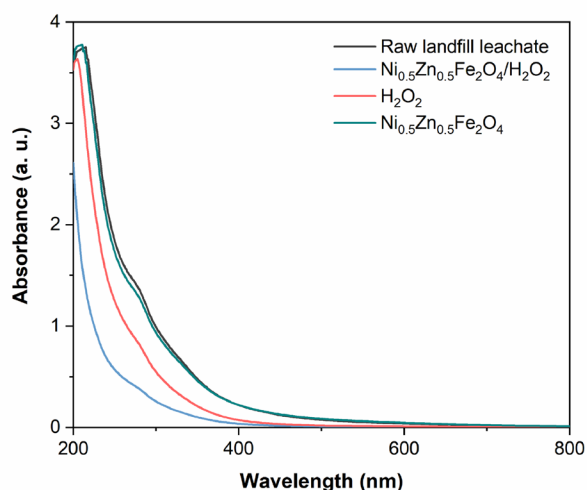


Figure 7 – UV-Vis spectrophotometric profiles of stabilized raw landfill leachate treated by different processes (samples diluted 20x: 0.5 mL of sample and 9.5 mL of distilled water).

The UV-Vis spectrophotometric profiles (Figure 7) of the raw leachate samples and those treated by different processes revealed that H_2O_2 had a significant influence; however, the presence of the $\text{Ni}_{0.5}\text{Zn}_{0.5}\text{Fe}_2\text{O}_4$ catalyst in the heterogeneous Fenton system enhanced the reactions and resulted in a treated leachate with a lower integrated spectral area than that obtained when the leachate was treated with H_2O_2 alone. The higher efficiencies achieved by the heterogeneous Fenton process ($\text{Ni}_{0.5}\text{Zn}_{0.5}\text{Fe}_2\text{O}_4/\text{H}_2\text{O}_2$) compared to the other processes were likely due to the synergy among the Ni, Zn, and Fe oxides in the $\text{Ni}_{0.5}\text{Zn}_{0.5}\text{Fe}_2\text{O}_4$ structure, owing to the characteristic electron mobility of mixed metal oxides, which increases the efficiency of redox reactions (Dantas et al., 2021b).

Conclusions

The vibrational analysis by FTIR confirmed the formation of the typical spinel structure of the $\text{Ni}_{0.5}\text{Zn}_{0.5}\text{Fe}_2\text{O}_4$ ferrite, and its characterization by XRD indicated that the material is composed of nanocrystallites with an average size of $36.93 \pm 1.36 \text{ nm}$. The micrographs obtained by SEM revealed agglomerates with irregular morphologies, consistent with the clustering of the nanocrystallites. The textural characterization by N_2 adsorption (BET-BJH) revealed a specific surface area of $64.17 \pm 1.07 \text{ m}^2 \text{ g}^{-1}$ and an average equivalent diameter of $17.44 \pm 0.29 \text{ nm}$. The DLS analysis provided an average particle size of $40.55 \pm 0.22 \text{ nm}$. Therefore, the synthesized $\text{Ni}_{0.5}\text{Zn}_{0.5}\text{Fe}_2\text{O}_4$ ferrite can be classified as a nanocatalyst. These properties enhanced the exposure of active sites during the heterogeneous Fenton process, which improved its efficiency.

In the investigation of the heterogeneous Fenton process ($\text{Ni}_{0.5}\text{Zn}_{0.5}\text{Fe}_2\text{O}_4/\text{H}_2\text{O}_2$) for the treatment of stabilized landfill leachate, the application of the CCD combined with RSM enabled the development of a mathematical model with an R^2 of 0.96 and the determination of optimal process conditions, considering the synergistic effects of the input variables ($\text{pH}=8.02$, H_2O_2 factor=1.14, and catalyst concentration= 0.66 g L^{-1}). The experimental validation of the model showed a satisfactory fit, indicating that the proposed model can be used for predictive purposes within the range investigated in the CCD.

The pH was the most statistically significant variable for leachate decolorization, followed by the H_2O_2 factor and the interaction between these two variables, respectively, whereas the catalyst concentration showed the least statistical influence on the response. Both pH and the H_2O_2 factor had a positive effect on the treatment, meaning that their higher levels led to increased efficiency, and the interaction between these variables synergistically enhanced leachate decolorization.

Considering the removal of simple aromatic compounds (absorbances at 228, 254, and 284 nm) and conjugated compounds (absor-

bance at 310 nm), as well as the integrated spectral area from 200 to 800 nm, the removal of all analyzed parameters followed the order: $\text{Ni}_{0.5}\text{Zn}_{0.5}\text{Fe}_2\text{O}_4/\text{H}_2\text{O}_2 > \text{H}_2\text{O}_2 > \text{Ni}_{0.5}\text{Zn}_{0.5}\text{Fe}_2\text{O}_4$. This outcome elucidated the effectiveness of the heterogeneous Fenton process in the decolorization of landfill leachate and in the removal of recalcitrant substances present in the stabilized leachate that absorb UV light at 228, 254, 284, and 310 nm. Therefore, considering the investigated parameters, the heterogeneous Fenton process was effective in the treatment of stabilized raw landfill leachate.

Authors' Contributions

Quirino, A. G. C.: Conceptualization, data curation, formal analysis, investigation, methodology, software, validation, visualization, writing—original draft, and writing—review and editing. **Dantas**, J.: Data curation, formal analysis, funding acquisition, resources, validation, writing—review and editing. **Cahino**, A. M.: Investigation. **Vidal**, I. C. A.: Investigation. **Bezerra**, F. C.: Investigation. **Rocha**, E. M. R.: Conceptualization, funding acquisition, project administration, resources, supervision, validation, and writing—review and editing.

References

- APHA; AWWA; WEF, 2012. Standard Methods for the Examination of Water and Wastewater. 22 ed. APHA, Washington, D.C.
- Bogacki, J.; Marcinowski, P.; El-Khozondar, B., 2019. Treatment of Landfill Leachates with Combined Acidification/Coagulation and The $\text{Fe}^0/\text{H}_2\text{O}_2$ Process. *Water*, v. 11 (2), 194. <https://doi.org/10.3390/w11020194>
- Chelladurai, S.J.S.; Murugan, K.; Ray, A.P.; Upadhyaya, M.; Narasimharaj, V.; Gnanasekaran, S., 2021. Optimization of process parameters using response surface methodology: A review. *Materials Today: Proceedings*, v. 37 (2), 1301-1304. <https://doi.org/10.1016/j.matpr.2020.06.466>
- Chen, W.; Zhang, A.; Gu, Z.; Li, Q., 2018. Enhanced degradation of refractory organics in concentrated landfill leachate by $\text{Fe}^0/\text{H}_2\text{O}_2$ coupled with microwave irradiation. *Chemical Engineering Journal*, v. 354, 680-691. <https://doi.org/10.1016/j.cej.2018.08.012>
- Colombo, A.; Módenes, A.N.; Trigueros, D.E.G.; Medeiros, B.L.; Marin, P.; Monte Blanco, S.P.D.; Hinterholz, C.L., 2018. Toxicity evaluation of the landfill leachate after treatment with photo-Fenton, biological and photo-Fenton followed by biological processes. *Journal of Environmental Science and Health, Part A*, v. 54 (4), 269-276. <https://doi.org/10.1080/10934529.2018.1544475>
- Correa, J.S.; Campos, M.; Montanhez, B.E.; Gonçalves, F.V.; Ide, C.N., 2020. Uso de Resposta Espectral em comprimentos de onda (230~290) nm como parâmetro indireto quantitativo de COD e DQO. *Revista DAE*, v. 68 (225), 51-62. <https://doi.org/10.36659/dae.2020.052>
- Dantas, J.; Leal, E.; Costa, A.C.F.M., 2021a. A reação de combustão: uma abordagem técnica das principais generalidades. In: Costa, A.C.F.M.; Dantas, J. (Eds.), *Nanomateriais cerâmicos por reação de combustão*. Poisson, Belo Horizonte, pp. 8-37. <https://doi.org/10.36229/978-65-5866-149-8>
- Dantas, J.; Leal, E.; Mapossa, A.B.; Pontes, J.R.M.; Freitas, N.L.; Fernandes, P.C.R.; Costa, A.C.F.M., 2021b. Biodiesel production on bench scale from different sources of waste oils by using NiZn magnetic heterogeneous nanocatalyst. *International Journal of Energy Research*, v. 45, 10924-10945. <https://doi.org/10.1002/er.6577>
- Ertugay, N.; Kocakaplan, N.; Malkoç, E., 2017. Investigation of pH effect by Fenton-like oxidation with ZVI in treatment of the landfill leachate. *International Journal of Mining, Reclamation and Environment*, v. 31 (6), 404-411. <https://doi.org/10.1080/17480930.2017.1336608>
- Guo, C.; Qin, X.; Guo, R.; Lv, Y.; Li, M.; Wang, Z.; Li, T., 2021. Optimization of heterogeneous Fenton-like process with Cu-Fe@CTS as catalyst for degradation of organic matter in leachate concentrate and degradation mechanism research. *Waste Management*, v. 134, 220-230. <https://doi.org/10.1016/j.wasman.2021.08.021>
- Guo, Y.; Wang, S.; Chi, C.; Wang, Y.; Gao, X.; Li, P.; Wang, Y.; Wan, C.; Wu, S., 2024. Treatment of mature landfill leachate using chemical and electrical Fenton with novel Fe-loaded GAC heterogeneous catalysts. *Journal of Water Process Engineering*, v. 60, 105169. <https://doi.org/10.1016/j.jwpe.2024.105169>
- Gutberlet, J.; Bramryd, T., 2025. Reimagining urban waste management: Addressing social, climate, and resource challenges in modern cities. *Cities*, v. 156, 105553. <https://doi.org/10.1016/j.cities.2024.105553>
- Harzali, H.; Azizi, M., 2024. Investigating the adsorption of Malachite green and Methyl green onto synthesized $\text{Ni}_{0.5}\text{Zn}_{0.5}\text{Fe}_2\text{O}_4$ spinel ferrites. *Journal of Environmental Chemical Engineering*, v. 12 (5), 113413. <https://doi.org/10.1016/j.jece.2024.113413>
- He, J.; Yang, X.; Men, B.; Wang, D., 2016. Interfacial mechanisms of heterogeneous Fenton reactions catalyzed by iron-based materials: A review. *Journal of Environmental Sciences*, v. 39, 97-109. <https://doi.org/10.1016/j.jes.2015.12.003>
- Klung, H.; Alexander, L., 1962. X-ray diffraction procedures. Wiley, New York.
- Li, P.; Yin, Z.; Chi, C.; Wang, Y.; Wang, Y.; Liu, H.; Lv, Y.; Jiang, N.; Wu, S., 2024. Treatment of membrane-concentrated landfill leachate by heterogeneous chemical and electrical Fenton processes with Iron-loaded granular activated carbon catalysts. *Journal of Environmental Chemical Engineering*, v. 12 (2), 112337. <https://doi.org/10.1016/j.jece.2024.112337>

- Lucena, L.G.; Rocha, E.M.R.; Porto, C.A.; Carvalho, N.A.; Silva, F.L.H., 2019. Multi-response optimisation of the solar photo-Fenton process for landfill leachate post-treatment. *Desalination and Water Treatment*, v. 151, 106-116. <https://doi.org/10.5004/dwt.2019.23754>
- Ma, C.; He, Z.; Jia, S.; Zhang, X.; Hou, S., 2018. Treatment of stabilized landfill leachate by Fenton-like process using Fe_3O_4 particles decorated Zr-pillared bentonite. *Ecotoxicology and Environmental Safety*, v. 161, 489-496. <https://doi.org/10.1016/j.ecoenv.2018.06.031>
- Mapossa, A.B.; Dantas, J.; Costa, A.C.F.M., 2020. Transesterification reaction for biodiesel production from soybean oil using $\text{Ni}_{0.5}\text{Zn}_{0.5}\text{Fe}_2\text{O}_4$ nanomagnetic catalyst: Kinetic study. *International Journal of Energy Research*, v. 44, 6674-6684. <https://doi.org/10.1002/er.5403>
- Metcalfe, Eddy, 2016. Tratamento de Efluentes e Recuperação de Recursos. Tradução de Ivanildo Hespagnol e José Carlos Mierzwa. AMGH, Porto Alegre.
- Moravia, W.G., 2010. Avaliação do tratamento de lixiviado de aterro sanitário através de processo oxidativo avançado conjugado com sistema de separação por membranas. Tese de Doutorado, Escola de Engenharia, Universidade Federal de Minas Gerais, Belo Horizonte. Retrieved 2025-08-12, from <http://hdl.handle.net/1843/ENGD-89WPAG>
- Moretti, A.C.L.; Santos, M.G.G.; Soares, M.E.; Freitas, J.V.R.; Rios, L.; Silva, F.S.; Gimenes, R.; Kondo, M.M.; Silva, M.R.A., 2023. Degradation of Municipal Solid Waste Landfill Leachate Using Ferrites from Spent Batteries as Heterogeneous Solar Photo-Fenton Catalyst. *International Journal of Environmental Research*, v. 17, 33. <https://doi.org/10.1007/s41742-023-00519-9>
- Myers, R.H.; Montgomery, D.C.; Anderson-Cook, C.M., 2016. Response surface methodology: process and product optimization using designed experiments. John Wiley & Sons, Hoboken.
- Neves, L.C.; Souza, J.B.; Vidal, C.M.S.; Herbert, L.T.; Souza, K.V.; Martins, K.G.; Young, B.J., 2020. Phytotoxicity indexes and removal of color, COD, phenols and ISA from pulp and paper mill wastewater post-treated by UV/ H_2O_2 and photo-Fenton. *Ecotoxicology and Environmental Safety*, v. 202, 110939. <https://doi.org/10.1016/j.ecoenv.2020.110939>
- Nguyen, D.-M.T.; Robinson, D.T.; Zurbrugg, C.; Nguyen, T.H.T.; Dang, H.-L.; Pham, V.-M., 2025. Strategic landfill site selection for sustainable waste management in Phu Yen Province, Vietnam using geospatial technologies. *Ecological Informatics*, v. 89, 103198. <https://doi.org/10.1016/j.ecoinf.2025.103198>
- Niveditha, S.V.; Gandhimathi, R., 2020a. Flyash augmented Fe_3O_4 as a heterogeneous catalyst for degradation of stabilized landfill leachate in Fenton process. *Chemosphere*, v. 242, 125189. <https://doi.org/10.1016/j.chemosphere.2019.125189>
- Niveditha, S.V.; Gandhimathi, R., 2020b. Mineralization of stabilized landfill leachate by heterogeneous Fenton process with RSM optimization. *Separation Science and Technology*, v. 56 (3), 567-576. <https://doi.org/10.1080/01496395.2020.1725573>
- Nouri, B.M.Y.; Al-Khatib, I.A., 2025. Exploring the energy recuperation and economic aspects of the waste stream at the Al-Minyah sanitary landfill in Palestine. *Cleaner Waste Systems*, v. 11, 100325. <https://doi.org/10.1016/j.clwas.2025.100325>
- Oliveira, D.M.; Andrada, A.S., 2019. Synthesis of ordered mesoporous silica MCM-41 with controlled morphology for potential application in controlled drug delivery systems. *Cerâmica*, v. 65 (374), 170-179. <https://doi.org/10.1590/0366-69132019653742509>
- Pham, V.L.; Kim, D.G.; Ko, S.O., 2018. $\text{Cu@Fe}_3\text{O}_4$ core-shell nanoparticle-catalyzed oxidative degradation of the antibiotic oxytetracycline in pre-treated landfill leachate. *Chemosphere*, v. 191, p. 639-650. <https://doi.org/10.1016/j.chemosphere.2017.10.090>
- Primo, O.; Rivero, M. J.; Ortiz, I., 2008. Photo-Fenton process as an efficient alternative to the treatment of landfill leachates. *Journal of Hazardous Materials*, v. 153 (1-2), 834-842. <https://doi.org/10.1016/j.jhazmat.2007.09.053>
- Quirino, A.G.C.; Rocha, E.M.R.; Cahino, A.M., 2022. Abordagem sistemática para identificação de lacunas no tratamento de lixiviados de aterros sanitários pelos processos Fenton e foto-Fenton heterogêneos. *Revista AIDIS de Ingeniería y Ciencias Ambientales: Investigación, Desarrollo y Práctica*, v. 15 (3), 1516-1540. <https://doi.org/10.22201/iingen.0718378xe.2022.15.3.81747>
- Reed, J.S., 1996. Principles of ceramics processing. John Wiley & Sons, New York, 2. ed.
- Sossou, K.; Prasad, S.B.; Agbotsou, K.E.; Souley, H.S.; Mudigandla, R., 2024. Characteristics of landfill leachate and leachate treatment by biological and advanced coagulation process: Feasibility and effectiveness – An overview. *Waste Management Bulletin*, v. 2 (2), 181-198. <https://doi.org/10.1016/j.wmb.2024.04.009>
- Sruthi, T.; Gandhimathi, R.; Ramesh, S.T.; Nidheesh, P.V., 2018. Stabilized landfill leachate treatment using heterogeneous Fenton and electro-Fenton processes. *Chemosphere*, v. 210, 38-43. <https://doi.org/10.1016/j.chemosphere.2018.06.172>
- Tahar, L.B.; Abualreish, M.J.A.A.E.; Noubigh, A., 2024. Optimization of reaction variables in the sol-gel synthesis of $\text{Ni}_{0.5}\text{Zn}_{0.5}\text{Fe}_2\text{O}_4$ nanoparticles as a very fast adsorbent of methylene blue. *Desalination and Water Treatment*, v. 317, 100052. <https://doi.org/10.1016/j.dwt.2024.100052>
- Taşci, S.; Özgüven, A.; Yildiz, B., 2021. Multi-response/multi-step optimization of heterogeneous fenton process with Fe_3O_4 catalyst for the treatment of landfill leachate. *Water, Air, & Soil Pollution*, v. 232, 275. <https://doi.org/10.1007/s11270-021-05225-w>
- Tejera, J.; Miranda, R.; Hermosilla, D.; Urrea, I.; Negro, C.; Blanco, Á., 2019. Treatment of a mature landfill leachate: comparison between homogeneous and heterogeneous photo-Fenton with different pretreatments. *Water*, v. 11 (9), 1849. <https://doi.org/10.3390/w11091849>
- Tizaoui, C.; Bouselmi, L.; Mansouri, L.; Ghrabi, A., 2007. Landfill leachate treatment with ozone and ozone/hydrogen peroxide systems. *Journal of Hazardous Materials*, v. 140 (1-2), 316-324. <https://doi.org/10.1016/j.jhazmat.2006.09.023>
- Turk, S.; Asci, Y., 2023. Color and chemical oxygen demand removal using homogeneous and heterogeneous Fenton oxidation of sugar industry wastewater. *Desalination and Water Treatment*, v. 306, 112-121. <https://doi.org/10.5004/dwt.2023.29825>
- Wang, Q.; Hou, X.; Liu, S.; Wang, Y.; Gu, S.; Zhou, G.; Chai, J., 2024. Rambutan-like $\text{Ni}_{0.5}\text{Zn}_{0.5}\text{Fe}_2\text{O}_4$ nanospheres with tunable N-doped carbon shell as anode materials for high performance lithium-ion batteries. *Journal of Alloys and Compounds*, v. 978, 173529. <https://doi.org/10.1016/j.jallcom.2024.173529>
- Wijekoon, P.; Koliyabandara, P.A.; Cooray, A.T.; Lam, S.S.; Athapattu, B.C.L.; Vithanage, M., 2022. Progress and prospects in mitigation of landfill leachate pollution: Risk, pollution potential, treatment and challenges. *Journal of Hazardous Materials*, v. 421, 126627. <https://doi.org/10.1016/j.jhazmat.2021.126627>